J. Fluid Mech. (2019), *vol.* 874, *pp.* 210–234.
doi:10.1017/jfm.2019.445

Swimming sheet in a density-stratified fluid

Rajat Dandekar[1], **Vaseem A. Shaik**[1] **and Arezoo M. Ardekani**[1,†]

[1]School of Mechanical Engineering, Purdue University, West Lafayette, IN 47907, USA

(Received 14 December 2018; revised 25 May 2019; accepted 26 May 2019;
first published online 4 July 2019)

In this work, we theoretically investigate the swimming velocity of a Taylor swimming sheet immersed in a linearly density-stratified fluid. We use a regular perturbation expansion approach to estimate the swimming velocity up to second order in wave amplitude. We divide our analysis into two regimes of low ($\ll O(1)$) and finite Reynolds numbers. We use our solution to understand the effect of stratification on the swimming behaviour of organisms. We find that stratification significantly influences motility characteristics of the swimmer such as the swimming speed, hydrodynamic power expenditure, swimming efficiency and the induced mixing, quantified by mixing efficiency and diapycnal eddy diffusivity. We explore this dependence in detail for both low and finite Reynolds number and elucidate the fundamental insights obtained. We expect our work to shed some light on the importance of stratification in the locomotion of organisms living in density-stratified aquatic environments.

Key words: propulsion, stratified flows, swimming/flying

1. Introduction

Density stratification in oceans and lakes occurs due to gradients in temperature or salinity. This affects the swimming behaviour and the migration patterns of organisms living in these environments (Doostmohammadi, Stocker & Ardekani 2012; Ardekani, Doostmohammadi & Desai 2017). An example of this includes the accumulation of dinoflagellates at thermoclines caused by restriction to propulsion due to steep thermal gradients (Heaney & Eppley 1981). Planktonic species of copepods have been observed to migrate towards higher salinity gradients and eventually concentrate at haloclines (Heuch 1995). Temperature-induced stratification has been shown to influence the distribution of the phytoplankton community (Arrigo *et al.* 1999) and even enhance the period of phytoplankton blooms (Sherman *et al.* 1998; Mahadevan *et al.* 2012).

The swimming of organisms in homogeneous fluids has been studied for over five decades (see Brennen & Winet 1977; Lauga & Powers 2009; Elgeti, Winkler & Gompper 2015; Lauga 2016) and significant progress has been made. Theoretical work in this direction was started by Taylor (1951) who derived an analytical expression for the swimming velocity of a thin waving sheet immersed in a homogeneous fluid at low Reynolds numbers. Later, Reynolds (1965) derived an expression for the sheet's swimming velocity by including the effect of inertia in his analysis. The formula was corrected by Tuck (1968), who showed that contrary to the observations made by Reynolds, the sheet swimming velocity decreases with inertia.

† Email address for correspondence: ardekani@purdue.edu

In the present work, we provide a theoretical analysis of the swimming velocity of a Taylor sheet in a density-stratified fluid. The theoretical approach used in this study has been applied by researchers in a wide range of physical scenarios. This includes locomotion in complex fluids (Chaudhury 1979; Lauga 2007; Elfring & Goyal 2016), in a gel (Leshansky 2009; Fu, Shenoy & Powers 2010), in two-phase viscous fluids (Du *et al.* 2012), in a liquid crystal (Krieger, Dias & Powers 2015) and near solid boundaries (Reynolds 1965; Katz 1974). Hydrodynamic interaction between multiple sheets is also studied using this methodology (Elfring & Lauga 2009). Despite the numerous ecological implications of stratification, there are limited theoretical studies which shed light on the swimming behaviour of microorganisms in a density-stratified environment.

Ardekani & Stocker (2010) quantified the effect of stratification on the swimming of organisms by means of singularity solutions at low Reynolds numbers. They identified the appropriate length scale to quantify the role of stratification and showed that stratification has a significant influence on the hydrodynamics of aquatic organisms. Point-force singularities, however, only give knowledge about the far-field flow generated by a swimmer at low Reynolds and Péclet numbers.

Numerical models were further developed for a more accurate representation of swimming organisms in density-stratified fluids. Doostmohammadi *et al.* (2012) carried out a detailed numerical analysis of the motion of a spherical squirmer swimming in a stratified fluid at low Reynolds numbers. They observed that buoyancy forces induced by density stratification have a significant impact on the flow field of the swimmer and its energy expenditure. They found the propulsion speed of the swimmer to be dependent on the direction of the thrust generation by the swimmer, which is generally not the case in homogeneous fluids. Wang & Ardekani (2015) performed three-dimensional fully resolved simulations of a suspension of squirmers in a density-stratified environment to study the mixing induced by organisms in aquatic environments.

Swimmers create a local disruption in the surrounding fluid during their locomotion. Biogenic mixing has been extensively studied in the literature (Katija 2012; Simoncelli, Thackeray & Wain 2017). There are arguments both in support of the importance of biogenic mixing (Dewar *et al.* 2006) and against it (Visser 2007). An understanding of the influence of stratification on the hydrodynamics of swimming is crucial for making reliable predictions about biogenic mixing.

In this work, we analytically derive an expression for the swimming velocity in a density-stratified fluid. We model the swimmer as a two-dimensional infinitely long sheet that propels by passing waves of small amplitude along its surface. This model can be used to represent the tail of a human spermatozoon (Taylor 1951), flat ciliated *Paramecium*, *Opalina* (Blake 1971) or *Caenorhabditis elegans* (Sznitman *et al.* 2010). We analyse the effects of stratification on swimmer propulsion. We divide our analysis into two regimes of low ($\ll O(1)$) and finite Reynolds numbers. This will help us understand how inertia affects the locomotion in a stratified fluid. Furthermore, we make predictions about the hydrodynamic power, swimming efficiency and the mixing induced by the swimmer in a stratified fluid.

2. Problem formulation

Figure 1 shows a schematic of a swimmer immersed in a linearly density-stratified fluid in the undisturbed state. The ambient or the undisturbed density variations in the fluid are given by

$$\rho_0 = \rho_\infty - \gamma y. \tag{2.1}$$

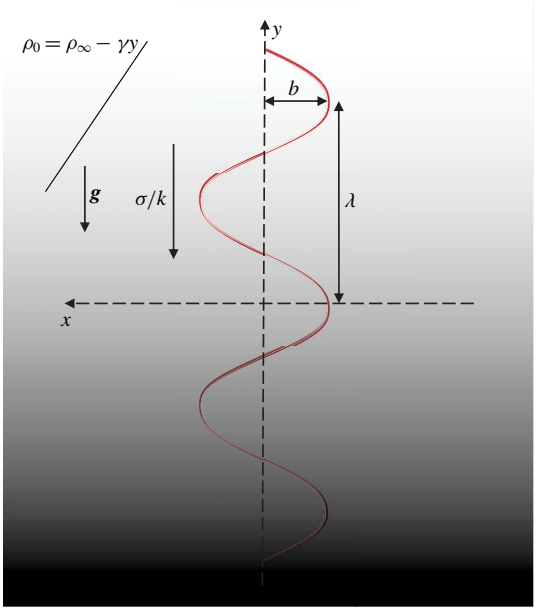

FIGURE 1. (Colour online) Swimming sheet immersed in a density-stratified fluid with ambient density $\rho_0 = \rho_\infty - \gamma y$, where gravity $\boldsymbol{g}$ points in the negative y direction. The swimmer propels in the y direction by generating a travelling wave in the negative y direction with a speed σ/k. Parameters b and λ are the wave amplitude and wavelength, respectively.

Here, ρ_∞ is the reference fluid density and $\gamma(>0)$ is the density gradient in the vertical direction.

We consider the swimmer to be neutrally buoyant with respect to the surrounding fluid. The swimmer is thus stationary when it does not propagate waves along its surface. This is a good assumption since marine organisms have been observed to regulate their density and remain neutrally buoyant in deep waters. For example, aquatic copepods, which are the dominant members of the zooplankton biomass, change their lipid concentration during winter to remain neutrally buoyant (Visser & Jónasdóttir 1999; Campbell & Dower 2003). Several species of notothenoid fishes in the mid-water community have been observed to be neutrally buoyant (Eastman 1985; Phleger 1998).

The swimmer propels by beating its flagella periodically, generating a travelling wave along its surface. This mechanism creates a disturbance in the surrounding fluid. The surface of the swimmer is assumed to deform according to the travelling wave $x = b\sin(ky + \sigma t)$, where b is the wave amplitude which is assumed to be small compared to the wavelength $2\pi/k$ (Taylor 1951) and σ is the angular frequency of the wave.

2.1. *Governing equations*

Using the Bousinessq approximation (Doostmohammadi *et al.* 2012; Ardekani *et al.* 2017), we begin by writing the equations of motion for the fluid:

$$\frac{\partial u}{\partial x} + \frac{\partial v}{\partial y} = 0, \tag{2.2}$$

$$\rho_\infty\left(\frac{\partial u}{\partial t}+u\frac{\partial u}{\partial x}+v\frac{\partial u}{\partial y}\right)=-\frac{\partial p}{\partial x}+\mu\left(\frac{\partial^2 u}{\partial x^2}+\frac{\partial^2 u}{\partial y^2}\right), \tag{2.3}$$

$$\rho_\infty\left(\frac{\partial v}{\partial t}+u\frac{\partial v}{\partial x}+v\frac{\partial v}{\partial y}\right)=-\frac{\partial p}{\partial y}-\rho g+\mu\left(\frac{\partial^2 v}{\partial x^2}+\frac{\partial^2 v}{\partial y^2}\right)-\rho_\infty\frac{\mathrm{d}V}{\mathrm{d}t}. \tag{2.4}$$

Equations (2.2)–(2.4) represent the continuity equation and the momentum conservation equations in the x and y directions, respectively. Here, u and v are the velocity fields in the x and y directions, respectively, in the frame of reference translating with the swimming velocity of the sheet given by V. Note that, in this frame of reference, the ambient density of the fluid (ρ_0) will depend on time.

When the changes in the concentration/temperature are linearly related to the changes in the density, one can solve for the advection–diffusion equation for the density (2.5), instead of such an equation for the temperature or concentration:

$$\frac{\partial \rho}{\partial t}+\frac{\partial(\rho u)}{\partial x}+\frac{\partial(\rho v)}{\partial y}=c\left(\frac{\partial^2 \rho}{\partial x^2}+\frac{\partial^2 \rho}{\partial y^2}\right). \tag{2.5}$$

Here, c is the diffusivity coefficient. The density and pressure fields can be expressed as a combination of disturbed and undisturbed fields: $\rho=\rho_0+\rho'$ and $p=p_0+p'$. Here, ρ' and p' are the disturbed density and pressure fields generated because of the deformation of the swimmer. The contribution of the undisturbed density to the buoyancy force term is balanced by the undisturbed pressure. Hence, we obtain the equations governing the flow and density in terms of the disturbance density and pressure as follows:

$$\frac{\partial u}{\partial x}+\frac{\partial v}{\partial y}=0, \tag{2.6}$$

$$\rho_\infty\left(\frac{\partial u}{\partial t}+u\frac{\partial u}{\partial x}+v\frac{\partial u}{\partial y}\right)=-\frac{\partial p'}{\partial x}+\mu\left(\frac{\partial^2 u}{\partial x^2}+\frac{\partial^2 u}{\partial y^2}\right), \tag{2.7}$$

$$\rho_\infty\left(\frac{\partial v}{\partial t}+u\frac{\partial v}{\partial x}+v\frac{\partial v}{\partial y}\right)=-\frac{\partial p'}{\partial y}-\rho' g+\mu\left(\frac{\partial^2 v}{\partial x^2}+\frac{\partial^2 v}{\partial y^2}\right)-\rho_\infty\frac{\mathrm{d}V}{\mathrm{d}t}, \tag{2.8}$$

$$\left(\frac{\partial \rho'}{\partial t}-\gamma V\right)+\frac{\partial(\rho' u)}{\partial x}+\frac{\partial(\rho' v)}{\partial y}-\gamma v=c\left(\frac{\partial^2 \rho'}{\partial x^2}+\frac{\partial^2 \rho'}{\partial y^2}\right). \tag{2.9}$$

Next, we non-dimensionalize the problem by using the following scales: length scale $l_c=1/k$, velocity scale $u_c=\sigma/k$, time scale $t_c=1/\sigma$, pressure scale $p_c=\mu\sigma$, density scale $\rho_c=\gamma/k$. The term $\partial V/\partial t$ will be non-dimensionalized later and is retained in its dimensional form for now. We use the same variables to denote the dimensionless variables. The governing equations are thus written as follows:

$$\frac{\partial u}{\partial x}+\frac{\partial v}{\partial y}=0, \tag{2.10}$$

$$Re\left(\frac{\partial u}{\partial t}+u\frac{\partial u}{\partial x}+v\frac{\partial u}{\partial y}\right)=-\frac{\partial p'}{\partial x}+\frac{\partial^2 u}{\partial x^2}+\frac{\partial^2 u}{\partial y^2}, \tag{2.11}$$

$$Re\left(\frac{\partial v}{\partial t}+u\frac{\partial v}{\partial x}+v\frac{\partial v}{\partial y}\right)=-\frac{\partial p'}{\partial y}-Ri\rho'+\frac{\partial^2 v}{\partial x^2}+\frac{\partial^2 v}{\partial y^2}-\frac{\rho_\infty}{\mu\sigma k}\frac{\mathrm{d}V}{\mathrm{d}t}, \tag{2.12}$$

$$Pe\left(\left(\frac{\partial \rho'}{\partial t}-V\right)+\frac{\partial(\rho' u)}{\partial x}+\frac{\partial(\rho' v)}{\partial y}-v\right)=\frac{\partial^2 \rho'}{\partial x^2}+\frac{\partial^2 \rho'}{\partial y^2}. \tag{2.13}$$

Here, $Re = \rho_\infty \sigma / k^2 \mu$ represents the Reynolds number, the ratio of the inertial to the viscous forces, $Pe = \sigma / k^2 c$ is the Péclet number, the ratio of the advective to the diffusive transport rates of density, and $Ri = \gamma g / \mu \sigma k^2$ is the viscous Richardson number, which is the ratio of the buoyancy to the viscous forces. The magnitude of the Richardson number represents the extent of stratification in the fluid.

The term $\partial V / \partial t$ denotes the dimensional acceleration of the swimmer. We expect the swimming velocity to change with time, because of the time-varying fluid density encountered by the translating sheet which is caused by the stratification gradient. The time-varying buoyancy force per unit volume experienced by the sheet (F_B) scales as

$$F_B \sim \frac{\gamma g}{k}. \tag{2.14}$$

If the density of the sheet is assumed to be ρ_p, the acceleration of the swimmer due to this buoyancy force will scale as

$$\frac{\mathrm{d}V}{\mathrm{d}t} \sim \frac{\gamma g}{\rho_p k}. \tag{2.15}$$

If we now substitute this scale for the sheet's acceleration in (2.12), we find that the unsteady force exerted on the fluid due to the translating swimming sheet satisfies

$$\frac{\rho_\infty}{\mu \sigma k} \frac{\mathrm{d}V}{\mathrm{d}t} = \frac{\rho_\infty}{\rho_p} Ri(a_s), \tag{2.16}$$

where a_s denotes the non-dimensional acceleration of the sheet. As a result, for steady motion of the sheet, the following condition must be satisfied:

$$\frac{\rho_\infty}{\rho_p} Ri(a_s) \ll 1. \tag{2.17}$$

As we have assumed the swimmer to be neutrally buoyant with respect to the surrounding fluid (density of the swimmer changes appropriately to ensure the net force acting on the swimmer is zero), we have

$$a_s \ll 1. \tag{2.18}$$

This implies that the unsteady contribution due to the sheet's translational velocity can be neglected and the motion of the sheet can be considered as steady. If the density of the swimmer remains constant with time, then the steady-state assumption is only valid if $Ri \ll 1$. We note that this assumption does not affect the calculation and analysis presented here as $\partial V / \partial t$ does not appear in the equation governing stream function. We expect, however, that the neutrally buoyant assumption is necessary to yield a consistent force balance condition.

We further simplify these expressions by representing the velocity fields in terms of the stream function (ψ) as follows:

$$u = -\frac{\partial \psi}{\partial y}, \quad v = \frac{\partial \psi}{\partial x}. \tag{2.19a,b}$$

Next, we eliminate the unknown pressure field by combining equations (2.11) and (2.12) to obtain a single equation in terms of the stream function. We make

another simplification by introducing a variable transformation given by $z = y + t$ (Reynolds 1965; Lauga 2007). This allows us to express the derivatives with respect to y and t in terms of a single variable z. We note that the wave appears to be steady in this transformed frame of reference. This allows us to express the governing equations with no dependence on the time variable. After performing these calculations, we finally obtain the equations of motion for the disturbances generated by the swimmer as follows:

$$\nabla^4\psi - Ri\frac{\partial\rho'}{\partial x} = Re\left(\frac{\partial\psi}{\partial x}\left(\frac{\partial}{\partial z}\nabla^2\psi\right) - \frac{\partial\psi}{\partial z}\left(\frac{\partial}{\partial x}\nabla^2\psi\right) + \frac{\partial}{\partial z}\nabla^2\psi\right), \tag{2.20}$$

$$Pe\left(\left(\frac{\partial\rho'}{\partial z} - V\right) + \frac{\partial}{\partial x}\left(-\rho'\frac{\partial\psi}{\partial z}\right) + \frac{\partial}{\partial z}\left(\rho'\frac{\partial\psi}{\partial x}\right) - \frac{\partial\psi}{\partial x}\right) = \frac{\partial^2\rho'}{\partial x^2} + \frac{\partial^2\rho'}{\partial z^2}. \tag{2.21}$$

Note that we have obtained a system of two differential equations in terms of two unknowns, the density field and the stream function.

2.2. *Boundary conditions*

We apply a no-slip and no-penetration boundary condition at the surface of the sheet which can be written as follows:

$$u|_{x=bk\sin(z)} = bk\cos(z), \quad v|_{x=bk\sin(z)} = 0. \tag{2.22a,b}$$

Far away from the sheet, the fluid velocity should be the negative of the sheet's swimming velocity:

$$u|_{x\to\infty} = 0, \quad v|_{x\to\infty} = -V. \tag{2.23a,b}$$

For the density field, we apply a no-flux boundary condition at the surface of the swimmer. For stratification induced due to gradients in concentration, this implies that the surface of the swimmer is impermeable; whereas it implies an adiabatic boundary condition at the surface in the case of thermal gradients. Hence we obtain

$$\boldsymbol{\nabla}\rho\cdot\boldsymbol{n}|_{x=bk\sin(z)} = 0. \tag{2.24}$$

Here, $\boldsymbol{n}$ represents the normal vector at the surface of the swimmer.

The disturbance density should vanish far away from the swimmer, which implies

$$\rho'|_{x\to\infty} = 0. \tag{2.25}$$

3. Solution

In order to solve equations (2.20) and (2.21), we expand the stream function and the density in the form of a regular perturbation series. We introduce the small parameter $\epsilon = bk$ and express the variables in the following form:

$$\psi = \epsilon\psi_1 + \epsilon^2\psi_2 + O(\epsilon^3), \quad \rho' = \epsilon\rho_1 + \epsilon^2\rho_2 + O(\epsilon^3). \tag{3.1a,b}$$

We express the swimming velocity of the sheet as

$$V = \epsilon V_1 + \epsilon^2 V_2 + O(\epsilon^3). \tag{3.2}$$

Next, we substitute these expansions in the boundary conditions and governing equations and solve at each order of ϵ.

3.1. *Boundary conditions for successive approximations*

We seek to transform the velocity boundary conditions at the surface to obtain conditions at $x=0$. Hence, we first expand the velocity boundary conditions at the surface of the swimmer about $x=0$ using Taylor series representation. We thus obtain

$$\left.\begin{aligned}\left.\frac{\partial\psi}{\partial z}\right|_{x=\epsilon\sin(z)} &= \left.\frac{\partial\psi}{\partial z}\right|_{x=0} + \epsilon\sin(z)\left.\frac{\partial^2\psi}{\partial z\partial x}\right|_{x=0} + \cdots,\\ \left.\frac{\partial\psi}{\partial x}\right|_{x=\epsilon\sin(z)} &= \left.\frac{\partial\psi}{\partial x}\right|_{x=0} + \epsilon\sin(z)\left.\frac{\partial^2\psi}{\partial x^2}\right|_{x=0} + \cdots.\end{aligned}\right\} \tag{3.3}$$

Next, we substitute the perturbation expansion for the stream function in the above expression and collect the terms at various powers of ϵ. We obtain the following boundary conditions at $x=0$ at the first and second order:

$$\frac{\partial\psi_1}{\partial x}=0, \quad \frac{\partial\psi_1}{\partial z}=-\cos(z) \quad \text{at } x=0, \tag{3.4a,b}$$

$$\frac{\partial\psi_2}{\partial x}=-\sin(z)\frac{\partial^2\psi_1}{\partial x^2}, \quad \frac{\partial\psi_2}{\partial z}=-\sin(z)\frac{\partial^2\psi_1}{\partial x\partial z} \quad \text{at } x=0. \tag{3.5a,b}$$

The no-flux boundary condition for density can be written as

$$\boldsymbol{\nabla}(\rho_0+\rho')\cdot\boldsymbol{n}|_{x=\epsilon\sin(z)}=0. \tag{3.6}$$

Using a similar procedure to that described for the velocity boundary conditions, we expand the above equation about $x=0$ to obtain

$$\boldsymbol{\nabla}(\rho_0+\rho')\cdot\boldsymbol{n}|_{x=\epsilon\sin(z)}=\boldsymbol{\nabla}(\rho_0+\rho')\cdot\boldsymbol{n}|_{x=0}+\epsilon\sin(z)\frac{\partial}{\partial x}(\boldsymbol{\nabla}(\rho_0+\rho')\cdot\boldsymbol{n})|_{x=0}. \tag{3.7}$$

The normal vector can also be represented by the Taylor series approximation to obtain

$$n_x=-1+\frac{\epsilon^2\cos^2(z)}{2}+O(\epsilon^3), \quad n_y=\epsilon\cos(z)+O(\epsilon^3). \tag{3.8}$$

Next, we substitute the density perturbation expansion in (3.7) and use the normal vector approximation to obtain the density boundary conditions at $x=0$ at the first and second order:

$$\frac{\partial\rho_1}{\partial x}=-\cos(z) \quad \text{at } x=0, \tag{3.9}$$

$$\frac{\partial\rho_2}{\partial x}=-\sin(z)\frac{\partial^2\rho_1}{\partial x^2}+\cos(z)\frac{\partial\rho_1}{\partial z} \quad \text{at } x=0. \tag{3.10}$$

Finally, the boundary condition for the vanishing disturbance density far away from the swimmer simplifies to

$$\rho_1\to 0, \quad \text{as } x\to\infty, \tag{3.11a}$$

$$\rho_2\to 0, \quad \text{as } x\to\infty. \tag{3.11b}$$

Next, we substitute the perturbation expansions of the velocity and the density fields in the equations of motion (equations (2.20) and (2.21)), and obtain the governing equations at various orders of ϵ.

3.2. *Solution at* $O(\epsilon)$

The equations governing the stream function and the density disturbance at $O(\epsilon)$ are given by

$$\nabla^4\psi_1 - Ri\left(\frac{\partial\rho_1}{\partial x}\right) = Re\left(\frac{\partial}{\partial z}\nabla^2\psi_1\right), \tag{3.12}$$

$$Pe\left(\left(\frac{\partial\rho_1}{\partial z} - V_1\right) - \frac{\partial\psi_1}{\partial x}\right) = \frac{\partial^2\rho_1}{\partial x^2} + \frac{\partial^2\rho_1}{\partial z^2}. \tag{3.13}$$

These equations are subjected to the boundary conditions at the first order (equations (3.4), (3.9) and (3.11*a*)). The first-order velocity averaged over the vertical direction at the sheet surface is zero (equation (3.4)). Thus, we expect the first-order solution to be periodic in the vertical direction. This allows us to express the stream function and the density in the following form:

$$\psi_1 = f(x)\mathrm{e}^{\mathrm{i}z}, \quad \rho_1 = g(x)\mathrm{e}^{\mathrm{i}z}. \tag{3.14a,b}$$

Consequently, we note that, in (3.13), the mean value of all the terms involving density (ρ_1) or the stream function (ψ_1) is zero. This implies that the first-order swimming velocity should be zero. Hence we get $V_1 = 0$. We thus conclude that stratification does not induce any velocity at the first order. Note that Taylor (1951) made a similar prediction for a sheet immersed in a homogeneous fluid.

Substituting these expressions in the governing equations at the first order and solving for $f(x)$, $g(x)$, we get the first-order fields as follows:

$$\psi_1 = \mathcal{R}((s_1\mathrm{e}^{m_1x} + s_2\mathrm{e}^{m_2x} + s_3\mathrm{e}^{m_3x})\mathrm{e}^{\mathrm{i}z}), \tag{3.15}$$

$$\rho_1 = \mathcal{R}\left(\left(s_1\frac{Pem_1}{1-m_1^2+\mathrm{i}Pe}\mathrm{e}^{m_1x} + s_2\frac{Pem_2}{1-m_2^2+\mathrm{i}Pe}\mathrm{e}^{m_2x} + s_3\frac{Pem_2}{1-m_3^2+\mathrm{i}Pe}\mathrm{e}^{m_3x}\right)\mathrm{e}^{\mathrm{i}z}\right). \tag{3.16}$$

Here $\mathcal{R}$ denotes the real part; m_1, m_2 and m_3 are the roots of the equation $m^6 + m^4(-3 - \mathrm{i}Pe - \mathrm{i}Re) + m^2(3 - PeRe + PeRi + \mathrm{i}(2Pe + 2Re)) - (1 + \mathrm{i}Pe)(1 + \mathrm{i}Re) = 0$ having a negative real part. Enforcing the boundary conditions at first order, we obtain the following equations whose solution determines s_1, s_2 and s_3:

$$\left.\begin{aligned} s_1 + s_2 + s_3 &= \mathrm{i}, \\ s_1m_1 + s_2m_2 + s_3m_3 &= 0, \\ s_1(m_1^2-1)^2 + s_2(m_2^2-1)^2 + s_3(m_3^2-1)^2 &= Ri. \end{aligned}\right\} \tag{3.17}$$

Hence,

$$\left.\begin{aligned} s_1 &= \frac{\begin{vmatrix} \mathrm{i} & 1 & 1 \\ 0 & m_2 & m_3 \\ Ri & (m_2^2-1)^2 & (m_3^2-1)^2 \end{vmatrix}}{D}, \quad s_2 = \frac{\begin{vmatrix} 1 & \mathrm{i} & 1 \\ m_1 & 0 & m_3 \\ (m_1^2-1)^2 & Ri & (m_3^2-1)^2 \end{vmatrix}}{D}, \\ s_3 &= \frac{\begin{vmatrix} 1 & 1 & \mathrm{i} \\ m_1 & m_2 & 0 \\ (m_1^2-1)^2 & (m_2^2-1)^2 & Ri \end{vmatrix}}{D}, \end{aligned}\right\} \tag{3.18}$$

where

$$D = \begin{vmatrix} 1 & 1 & 1 \\ m_1 & m_2 & m_3 \\ (m_1^2-1)^2 & (m_2^2-1)^2 & (m_3^2-1)^2 \end{vmatrix}. \tag{3.19}$$

3.3. *Solution at* $O(\epsilon^2)$

The equations governing the stream function and the density disturbance at $O(\epsilon^2)$ are given by

$$\nabla^4\psi_2 - Ri\left(\frac{\partial\rho_2}{\partial x}\right) = Re\left(\frac{\partial\psi_1}{\partial x}\left(\frac{\partial}{\partial z}\nabla^2\psi_1\right) - \frac{\partial\psi_1}{\partial z}\left(\frac{\partial}{\partial x}\nabla^2\psi_1\right) + \frac{\partial}{\partial z}\nabla^2\psi_2\right), \tag{3.20}$$

$$Pe\left(-V_2 + \frac{\partial\rho_2}{\partial z} + \frac{\partial}{\partial x}\left(-\rho_1\frac{\partial\psi_1}{\partial z}\right) + \frac{\partial}{\partial z}\left(\rho_1\frac{\partial\psi_1}{\partial x}\right) - \frac{\partial\psi_2}{\partial x}\right) = \frac{\partial^2\rho_2}{\partial x^2} + \frac{\partial^2\rho_2}{\partial z^2}. \tag{3.21}$$

From the boundary conditions at the second order (equations (3.5), (3.10) and (3.11*b*)), we find that second-order vertical velocity and the density gradient averaged in the vertical direction at the surface of the sheet are non-zero. Hence, the velocity and density fields must have a non-zero mean component to satisfy the boundary conditions. In order to obtain these mean components, we define the vertical averaged density and stream function in the domain as follows:

$$\langle\psi_2\rangle = \frac{1}{2\pi}\int_0^{2\pi}\psi_2(x, z)\,\mathrm{d}z, \quad \langle\rho_2\rangle = \frac{1}{2\pi}\int_0^{2\pi}\rho_2(x, z)\,\mathrm{d}z. \tag{3.22a,b}$$

We now average over the vertical direction on both sides of (3.20) and (3.21) to obtain

$$\frac{\mathrm{d}^4\langle\psi_2\rangle}{\mathrm{d}x^4} = Ri\frac{\mathrm{d}\langle\rho_2\rangle}{\mathrm{d}x} + Rek_1(x), \tag{3.23}$$

$$Pe\left(-V_2 + k_2(x) - \frac{\mathrm{d}\langle\psi_2\rangle}{\mathrm{d}x}\right) = \frac{\mathrm{d}^2\langle\rho_2\rangle}{\mathrm{d}x^2}. \tag{3.24}$$

Here, $k_1(x) = \langle\partial\psi_1/\partial x(\partial/\partial z\nabla^2\psi_1) - \partial\psi_1/\partial z(\partial/\partial x\nabla^2\psi_1)\rangle$ and $k_2(x) = \langle\partial/\partial x(-\rho_1\,\partial\psi_1/\partial z) + \partial/\partial z(\rho_1\partial\psi_1/\partial x)\rangle$, where $\langle.\rangle$ represents the average in the vertical direction. These can be easily obtained from the first-order velocity and density fields.

We define $\langle\psi_2\rangle = -V_2x + \psi_{2s}$, where $\partial\psi_{2s}/\partial x$ is the vertically averaged y-direction velocity field in the fluid domain measured in a stationary frame of reference. We substitute this expression in (3.23) and (3.24) to obtain the following differential equation for ψ_{2s} after some algebraic manipulations:

$$\frac{\mathrm{d}^5\psi_{2s}}{\mathrm{d}x^5} + (RiPe)\frac{\mathrm{d}\psi_{2s}}{\mathrm{d}x} = (RiPe)k_2(x) + Re\frac{\mathrm{d}}{\mathrm{d}x}k_1(x). \tag{3.25}$$

We can now find the contribution of the mean velocity field at $x = 0$, which is given by

$$\frac{\mathrm{d}\langle\psi_2\rangle}{\mathrm{d}x}(x=0) = -V_2 + \frac{\mathrm{d}\psi_{2s}}{\mathrm{d}x}(x=0). \tag{3.26}$$

We equate this contribution to the mean value of the second-order boundary condition at the sheet surface (equation (3.5*a*)) to obtain

$$V_2 = \left\langle \sin(z)\frac{\mathrm{d}^2\psi_1}{\mathrm{d}x^2}(x=0)\right\rangle + \frac{\mathrm{d}\psi_{2s}}{\mathrm{d}x}(x=0). \tag{3.27}$$

Here, ψ_1 and ψ_{2s} are obtained by solving equations (3.15) and (3.25), respectively. We solve equations (3.25) and (3.27) to obtain the velocity of the sheet which is given by

$$V_2 = \frac{1}{2}\mathrm{Im}\left(\sum_{i=1}^{3}\sum_{j=1}^{3}\frac{s_i\overline{s_j}(m_i^2-1)(m_i+\overline{m_j})}{RiPe+(m_i+\overline{m_j})^4}\left(Pe\frac{(m_i^2-1)^2}{m_i}-Re(m_i+\overline{m_j})\right)-\sum_{i=1}^{3}m_i^2 s_i\right), \tag{3.28}$$

where $\overline{s_i}$ and $\overline{m_i}$ represent the complex conjugates of s_i and m_i, respectively, Im is the imaginary part and $\mathrm{i}^2=-1$. The dimensional swimming velocity of the sheet is given by

$$V_s = \left(\frac{\sigma}{k}\right) b^2k^2V_2. \tag{3.29}$$

From the above expression, we observe that the velocity of a swimmer immersed in density-stratified fluid is proportional to the wave speed, the square of the wave amplitude and the wavenumber. By substituting $Ri = 0$ in (3.28), we obtain the expression for the sheet's swimming velocity in a homogeneous fluid as follows:

$$V_s = \left(\frac{\sigma}{k}\right) b^2k^2\left(\frac{1}{2}\sqrt{\frac{1+\sqrt{1+Re^2}}{2}}\right). \tag{3.30}$$

We note that this expression matches with the formula derived by Tuck (1968), thus verifying the theoretical procedure used in our analysis.

4. Results and discussion

We divide our analysis into two regimes. We first discuss the low-Reynolds-number regime, where the inertial forces acting on the swimmer are negligible ($Re \ll 1$). In this case, the swimmer is propelled only by the viscous forces acting on its surface. The second regime is that of a swimmer having a finite Re. Here, inertial forces can no longer be neglected and will contribute to the propulsion of the swimmer. Owing to the dearth of theoretical studies conducted in both these regimes, we expect our results to provide a fundamental understanding about the effect of stratification on the swimming of microorganisms.

Henceforth, we will express the Péclet number in terms of the Prandtl number ($Pr = Pe/Re$) which is defined as the ratio of the momentum diffusivity to the thermal diffusivity. We use the same number for salt transport as well, even though such a number is the Schmidt number when mass transfer occurs. Typical values of Prandtl number for some practically relevant stratification conditions are $Pr = 700$ for salt stratification in water and $Pr = 7$ for temperature-stratified water. The magnitude of stratification is often represented by the Brunt–Väisälä frequency ($N = \sqrt{\gamma g/\rho_\infty}$). The typical values of N range from 10^{-4} to 0.3 s^{-1} (Thorpe 2005). Using this estimate, in density-stratified water ($\rho_\infty \approx 1000$ kg m^{-3}, $\mu \approx 10^{-3}$ kg m^{-1} s^{-1}), we find that $\gamma \approx 10^{-6}$–10 kg m^{-4}. We can use these parameter values to determine typical values of $Re = \rho_\infty u_c l_c/\mu$ and $Ri = \gamma g l_c^3/(\mu u_c)$ for various motile organisms in stratified water with $\gamma = 1$ kg m^{-4}. Examples include *Escherichia coli*, *Salmonella typhimurium* ($l_c \approx 1$ μm, $u_c \approx$ 20–30 μm s^{-1}) (Lauga & Powers 2009): $Re \approx 10^{-5}$–10^{-4}, $Ri \approx 10^{-8}$; copepods ($l_c \approx 0.05$–0.3 cm, $u_c \approx 0.1$–0.5 cm s^{-1}) (Strickler 1975): $Re \approx 10^{-2}$–10^{3}, $Ri \approx 0.01$–0.05; *Euphausia pacifica* (krills) ($l_c \approx 1$ cm, $u_c \approx 5$ mm s^{-1}) (Yen, Brown & Webster 2003): $Re \approx 175$, $Ri \approx 1$–5.

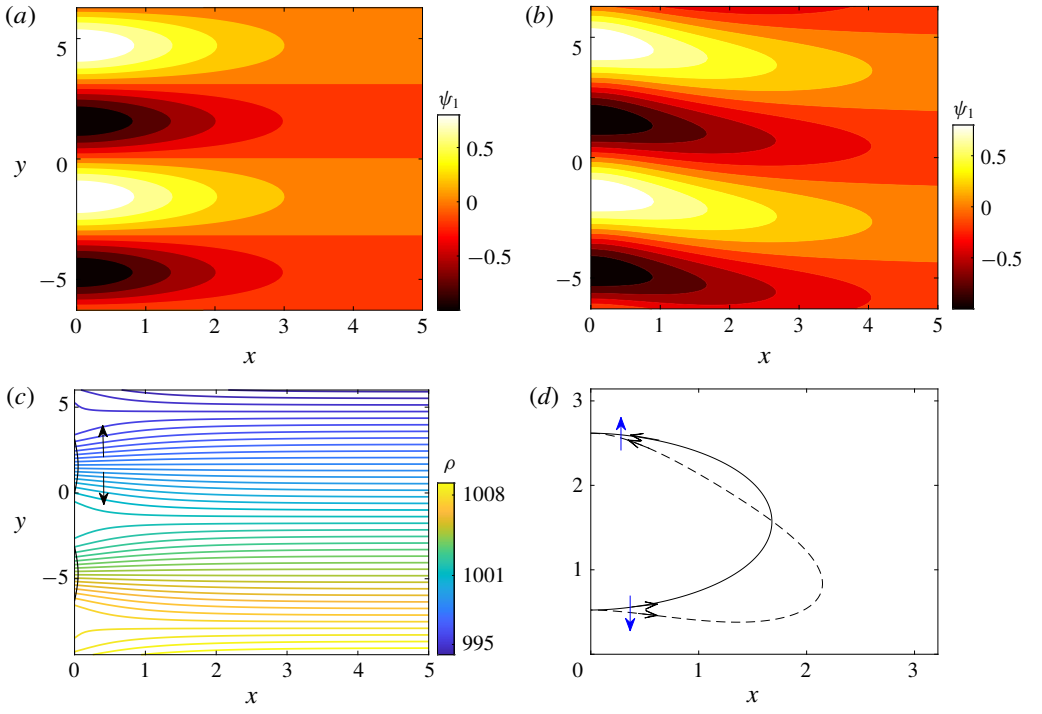

FIGURE 2. (Colour online) First-order flow field (ψ_1) induced by the swimmer in (*a*) homogeneous fluid and (*b*) stratified fluid ($Pr = 7$, $Ri = 5$). Contours are the streamlines and colours show the value of the stream function. (*c*) Isopycnals ($\rho = \rho_0 + \rho'$) for $Pr = 7$, $Ri = 5$. Vertical arrows represent the direction of isopycnal retreat and solid black lines represent the swimming sheet. (*d*) Comparison of streamline of a stratified fluid (dashed line) with a homogeneous fluid (solid line). Black arrows represent the direction of the first-order velocity and blue arrows represent additional vertical velocities due to isopycnal retreat. Here $Re = 0.001$ is chosen for all the subplots.

4.1. *Low-Reynolds-number regime* ($Re \ll 1$)

4.1.1. *Effect of stratification on swimming velocity*

We first analyse the first-order flow field generated by the propelling sheet in the presence of stratification. We observe that stratification markedly changes the flow pattern in comparison with the homogeneous fluid (figure 2*a*,*b*). The flow field generated by the sheet is vertically biased as the streamlines bend towards the denser portion of the fluid. This observation can be understood by considering that the motion of the swimmer disturbs the density field in its proximity. This causes the isopycnals to deform and assume a configuration which is no longer horizontal. Note that the isopycnals deform such that they are oriented in a direction normal to the surface of the swimmer, so as to satisfy the no-flux boundary condition. Consequently, the isopycnals near the lower (upper) end of the sheet's crest deflect in the positive (negative) y direction. This is clearly shown in figure 2(*c*) which depicts the displaced isopycnals close to the sheet. The tendency of the displaced density layers to return to their original position creates additional vertical velocities in the fluid domain (shown by vertical arrows in figure 2*c*), in a direction which is opposite to the deformation of isopycnals. We note that this velocity acts in the negative y direction near the lower

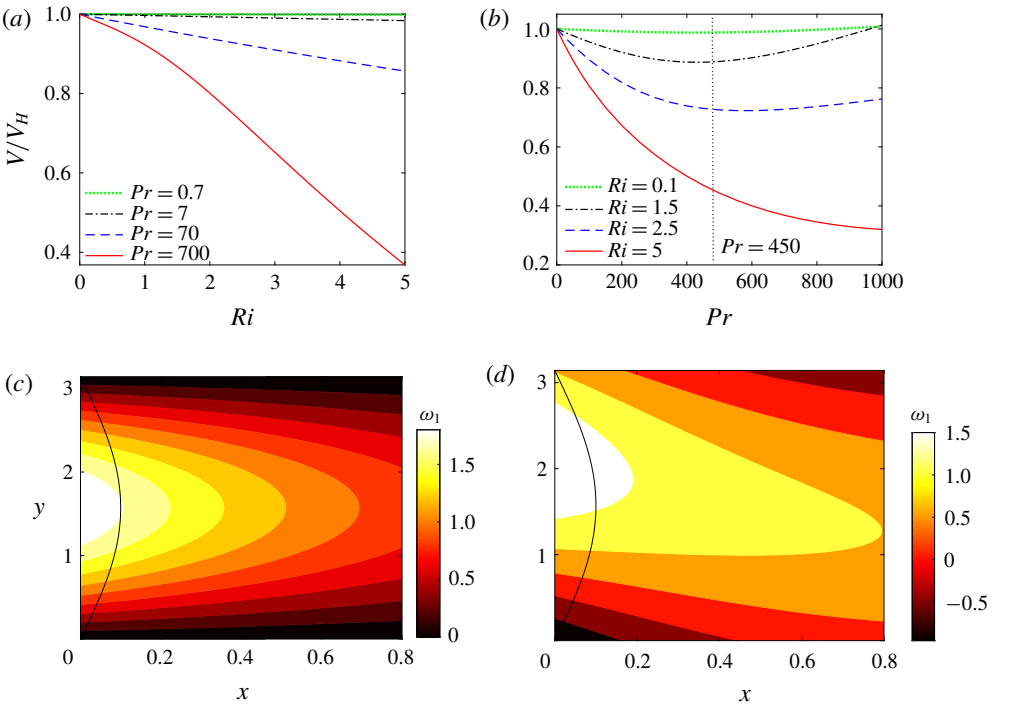

FIGURE 3. (Colour online) Variation of the swimming velocity with (*a*) Richardson number and (*b*) Prandtl number, for $Re = 0.001$, normalized with respect to the velocity in a homogeneous fluid in the Stokes regime. First order vorticity field at (*c*) $Ri = 0$ and (*d*) $Ri = 5$, for $Re = 0.001$, $Pr = 700$.

end of the sheet's crest ($0 \leqslant y < \pi/2$) and in the positive y direction near the upper end ($\pi/2 < y \leqslant \pi$). One can add this stratification-induced velocity to the flow field in a homogeneous fluid to determine the flow field in a stratified fluid. If we consider a streamline in a homogeneous fluid which is directed from $y \approx 0.5$ to $y \approx 2.5$ as shown by the solid curve in figure 2(*d*), the effect of stratification-induced velocity is to decrease the slope of this curve near $y \approx 0.5$ and to increase this slope near $y \approx 2.5$, due to which the streamline in a stratified fluid appears to be bent in the negative y direction. This flow pattern has a significant influence on the hydrodynamics of the sheet propulsion, which is discussed in later sections. The effect of stratification on swimming can be characterized by Ri which depends on the strength of the density stratification and Pr which depends on the diffusivity of the stratifying agent. We now analyse the effect of both of these parameters on the swimming velocity.

Figure 3(*a*) shows the variation of the swimming velocity with Ri normalized with respect to the velocity in a homogeneous fluid ($Ri = 0$, $Re = 0$). We observe that the velocity decreases with stratification for all values of Pr. This implies that an increase in stratification hampers the vertical motion of swimmers. We now observe the effect of diffusion on the swimming velocity (see figure 3*b*). For smaller levels of stratification, we see that the velocity initially decreases with Pr, and then increases after reaching a minimum (see figure 3*b* ($Ri = 1.5$)). Thus, for small Ri, diffusivity of the stratifying agent plays a key role in determining the swimming behaviour. For higher levels of stratification, we find that the velocity monotonically decreases

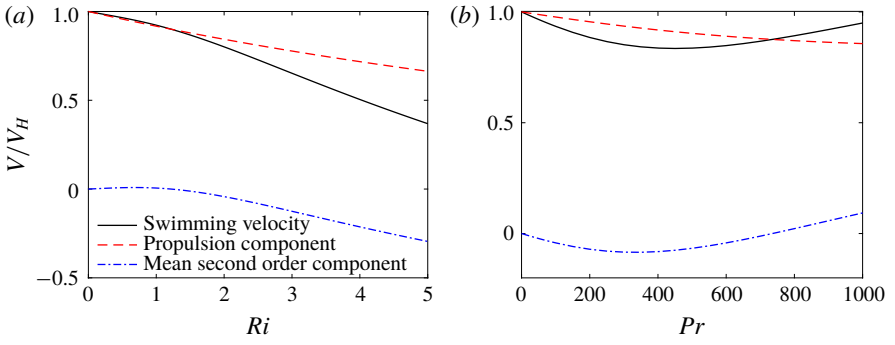

FIGURE 4. (Colour online) Decomposition of the swimming velocity for (*a*) $Pr = 700$ and (*b*) $Ri = 1.5$, for $Re = 0.001$.

with Pr (see figure 3*b* ($Ri = 5$)). Additionally, we observe that, for very high values of diffusion ($Pr \ll 1$), the swimmer moves with the same velocity as that in a homogeneous fluid (see figure 3*b*). This is mainly because the density disturbance becomes negligible for very high values of diffusion. We further find that, for small values of Ri and Pe, the velocity decreases linearly with respect to these parameters. By using a numerical fit to the velocity curves in figure 3(*a,b*) for small Ri and Pe, the mathematical form of the velocity variation is obtained as follows:

$$V = V_H(1 - 0.46RiPe). \tag{4.1}$$

The sheet swimming velocity can be decomposed into two contributions (refer to (3.27)). The first term signifies the second-order vertical velocity at the sheet boundary because of the no-slip condition at the sheet surface. In the case of a homogeneous fluid, this is the only contribution to the sheet propulsion. We can rewrite this term as follows:

$$\left\langle \sin(z)\frac{\mathrm{d}^2\psi_1}{\mathrm{d}x^2}(x=0)\right\rangle = \frac{1}{2}(\omega_1(0,\,\pi/2) - 1). \tag{4.2}$$

Here, $\omega_1(0,\,\pi/2)$ represents the value of first-order vorticity in the fluid at the sheet crests. We thus find that this contribution to the swimming velocity is directly proportional to the magnitude of the vorticity generated in the fluid at the sheet crests. Lauga & Powers (2009) explained that the vortices are caused due to the opposite direction of longitudinal displacement of the fluid particles close to the sheet's crests. The second contribution is caused by the mean second-order velocity field which is induced in the fluid when density stratification is taken into account (refer to (3.25)). For a stratified fluid without inertia this contribution is completely governed by $k_2(x)$. Physically, this quantity signifies average rate of mass transfer due to advection across the fluid volume.

Figure 4 shows the reconstruction of the velocity from both these contributions. We observe that the second-order vertical velocity at the sheet boundary (represented by the propulsion component) is positive for all Ri, Pr, which causes the sheet to propel. Furthermore, this propulsion component of the velocity decreases with Ri. We rationalize this observation by considering that the propulsion component is generated due to the vortices developed in the fluid at the sheet crests (refer to (4.2)).

Figure 3(*c*,*d*) shows the modification in the vorticity field when stratification is taken into account. We find that the vorticity peak is no longer aligned with the sheet crests in the presence of stratification. Consequently, the magnitude of the vorticity at the sheet crests decreases, which ultimately causes the propulsion component to decrease with Ri.

From figure 4(*a*), we also find that the contribution of the mean second-order velocity field developed in the fluid due to stratification is negative. In order to understand this observation, we first note that, as the swimmer translates in the positive y direction, it pulls the surrounding fluid with itself. If we now consider a fixed control volume inside the fluid, we deduce that its mass is increasing with time, as the fluid is being replaced by a heavier fluid. If we further assume that diffusion is not very large, then mass conservation dictates that the rate of mass transfer due to advection across the control volume should be negative. Consequently, we note that the quantity that governs the mean second-order velocity field (refer to $k_2(x)$ in (3.25)) is negative everywhere in the fluid domain. This causes the contribution of the mean second-order velocity field to oppose the propulsion of the swimmer. Furthermore, if the ambient density gradient is increased, the mass of the control volume will increase at a faster rate, causing $k_2(x)$ to become more negative in the fluid. Consequently, we find that increasing stratification leads to an increase in the opposition caused by the mean second-order velocity field (see figure 4*a*). After analysing the variations of both of the velocity contributions, we infer that increasing stratification restricts the vertical motion of swimmers. From figure 4(*b*), we observe that, for low stratification strengths, the propulsion component decreases with Pr; however, the resistance to propulsion increases with Pr and then decreases, eventually supporting the propulsion for high Pr. This trend is consequently reflected in the velocity of the swimmer (see figure 3*b*, $Ri = 1.5$). Interestingly, if the density gradient is small, for low levels of diffusion, the swimmer can even propel faster than in a homogeneous fluid (see figure 3*b*, $Ri = 1.5$, $Pr = 1000$).

To summarize, we find that higher stratification strengths mostly hamper the swimming velocity of the sheet in a low-Reynolds-number regime. This result is expected from an intuitive standpoint, because for the class of problems involving particles settling in a density-stratified Newtonian fluid, it is well known that an increased drag force inhibits their vertical motion (Yick *et al.* 2009; Candelier, Mehaddi & Vauquelin 2014; Doostmohammadi, Dabiri & Ardekani 2014). However, in the narrow regime of lower stratification strengths and negligible diffusion, we find that stratification supports the swimming motion of the sheet.

4.1.2. *Effect of stratification on power expenditure and swimming efficiency*

In this section, we analyse the influence of stratification on the power expended by the swimmer to achieve propulsion. This depends on the work done by the hydrodynamic stresses acting on its surface. Ardekani & Stocker (2010) predicted that point forces acting on a stratified fluid generate a flow field around the swimmer which augments its power expenditure. Later, Doostmohammadi *et al.* (2012) analysed the power expended by squirmers suspended in a density-stratified fluid. By conducting a series of numerical studies, they came to the same conclusion that stratification magnifies the energy required for swimming.

The power expended by the swimmer is given by

$$P = \int_{S(t)} \boldsymbol{n}\cdot\boldsymbol{\sigma}\cdot\boldsymbol{u}\,\mathrm{d}S = \int_{\mathcal{V}(t)} (\boldsymbol{\nabla}\cdot\boldsymbol{\sigma})\cdot\boldsymbol{u}\,\mathrm{d}\mathcal{V} + 2\mu\int_{V(t)} \boldsymbol{E}:\boldsymbol{E}\,\mathrm{d}\mathcal{V}. \tag{4.3}$$

Here, $\boldsymbol{\sigma}$ and $\boldsymbol{E}$ are the stress tensor and the rate-of-strain tensor, respectively, $S(t)$ represents the surface of the swimmer and $\mathcal{V}$ represents the fluid volume which is bounded by the sheet surface and extends to infinity. The first term on the right-hand side indicates the work done to move the isopycnals against gravity, while the second term indicates the viscous energy dissipation in the fluid. The rate-of-strain tensor can be written as $\boldsymbol{E} = \frac{1}{2}(\boldsymbol{\nabla u} + \boldsymbol{\nabla u}^{\mathrm{T}})$, where $\boldsymbol{u} = (u_1, v_1)$ represents the first-order velocity field. The divergence of the stress tensor is

$$\boldsymbol{\nabla} \cdot \boldsymbol{\sigma} = -\rho' \boldsymbol{g}. \tag{4.4}$$

We non-dimensionalize the above quantities and obtain the following expression for the power dissipation at low Reynolds numbers:

$$P = \int_{\mathcal{V}(t)} \mu\sigma^2 \left(\epsilon^2 \left(Ri(\rho_1 v_1) + 2\left(\left(\frac{\partial u_1}{\partial x} \right)^2 + \left(\frac{\partial v_1}{\partial z} \right)^2 + \frac{1}{2}\left(\frac{\partial u_1}{\partial z} + \frac{\partial v_1}{\partial x} \right)^2 \right) \right) + O(\epsilon^3) \right) \mathrm{d}\mathcal{V}. \tag{4.5}$$

Here, u_1 and v_1 are the first-order velocity fields in the x and y directions, respectively. We observe that, in addition to the viscous dissipation, stratification induces an additional contribution from the buoyancy force generated by the first-order disturbance density field.

We calculate the mean power over one time period and compare it with the power expended by the swimmer in a homogeneous fluid by varying the stratification magnitude (see figure 5*a*). We observe that stratification augments the power expenditure at all values of Pr considered. We previously noted that the streamlines surrounding the swimmer become more tilted in the presence of stratification (figure 2*b*). Similar to the streamlines, we find that the velocity contours also become vertically skewed due to stratification effects. The skewed velocity contours augment the velocity gradients generated in the fluid domain. This enhances the shear stresses developed in the fluid, and consequently the viscous dissipation in the fluid increases. Moreover, the swimmer consumes more energy in mixing the fluid as well. As a result, we find that swimming becomes more energetically expensive in a density-stratified fluid. This result matches with the predictions made by Ardekani & Stocker (2010) and Doostmohammadi *et al.* (2012), even though the geometry of the swimmer is different in each case. We further observe that an increase in diffusion decreases the power expenditure of the swimmer. This can be understood by considering that stronger diffusion counteracts the effect of buoyancy more effectively by restricting the tilting of the density contours. As a result, the work done by buoyancy forces is mitigated which consequently decreases the power expenditure. This analysis is shown in figure 5(*c*,*d*) which compares the isopyncal deflections for $Pr = 7$ and $Pr = 700$. In order to understand the deflection of isopycnals for low values of diffusion, we note that, far away from the swimmer, the vertically averaged mass flux developed in the fluid due to the deformation of the swimmer is positive for smaller values of diffusion. This implies that, as the swimmer propels, fluid mass is migrating in the positive y direction. To account for this mass transport, the isopycnals can no longer be horizontal and are bent upwards. However, for high values of diffusion, we find that there is no mass transport across the isopycnals and hence they retain their undisturbed position.

We seek to analyse the effect of stratification on the hydrodynamic efficiency of the swimmer. Efficiency depends on the fraction of the available power used for locomotion. Lighthill (1952) defined swimming efficiency as the ratio of external

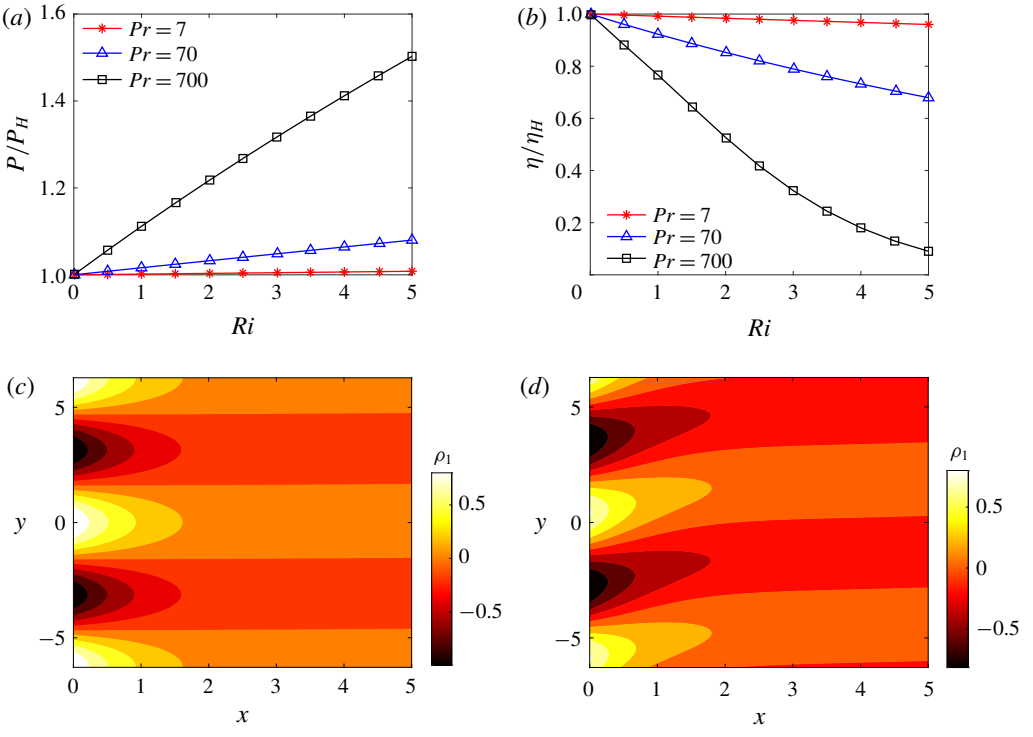

FIGURE 5. (Colour online) Effect of stratification on (*a*) power expenditure and (*b*) swimming efficiency, normalized with respect to that in a homogeneous fluid in the Stokes regime. First-order density field (ρ_1) contours for (*c*) $Ri = 5$, $Pr = 7$ and (*d*) $Ri = 5$, $Pr = 700$. Here $Re = 0.001$ is chosen for all the subplots.

power required to move the swimmer at a constant velocity to the power expended by the swimmer. This definition is commonly used to represent the hydrodynamic efficiency of undulating sheets. We use this definition to quantify the hydrodynamic efficiency in a stratified fluid. Hence, we obtain

$$\eta \propto \frac{V^2}{P}. \tag{4.6}$$

Here, V is the swimming velocity and P is the mean power expended by the swimmer over one time period. We compare this efficiency with that in the homogeneous fluid and observe the variation with the stratification strength (see figure 5*b*). We observe that an increase in Ri decreases the efficiency of the swimmer. This is expected because with increasing Ri, the power expenditure of the swimmer is increasing (see figure 5*a*), while the swimming velocity is decreasing (see figure 3*a*). Hence, the swimmer is converting less fraction of the available power into locomotion. For the values of Pr considered for the efficiency analysis, we have seen that with increasing diffusion, the swimming velocity increases, while the power expenditure of the sheet decreases. This causes the swimming efficiency to increase with diffusion for a fixed Ri.

4.1.3. *Effect of stratification on mixing*

Biogenic mixing has been studied via experimental and numerical studies (Katija & Dabiri 2009; Katija 2012; Wang & Ardekani 2015). Mixing efficiency can be defined

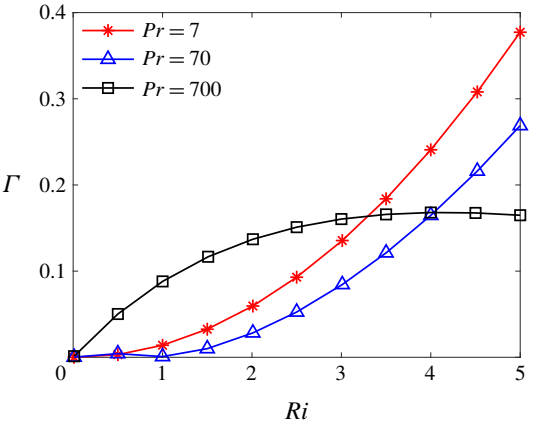

FIGURE 6. (Colour online) Variation of the mixing efficiency with Richardson number for $Re = 0.001$.

as the fraction of mechanical energy converted to change the potential energy of the fluid by the mixing process. It is represented by the following formula:

$$\Gamma = \frac{\Delta PE}{\Delta KE} = \frac{Ri \int_{\mathcal{V}} \rho' v \, \mathrm{d}\mathcal{V}}{Ri \int_{\mathcal{V}} \rho' v \, \mathrm{d}\mathcal{V} + 2 \int_{\mathcal{V}} \boldsymbol{E} : \boldsymbol{E} \, \mathrm{d}\mathcal{V}}. \tag{4.7}$$

Here, ρ' and v denote the disturbance density field and the vertical velocity field, respectively. The numerator denotes the potential energy change in the fluid induced by the swimming organism, while the denominator indicates the total mechanical energy of the fluid. From the above expression, it is evident that mixing efficiency depends on the ratio of the change in the potential energy of the fluid to the viscous dissipation.

Figure 6 shows the variation of mixing efficiency with Ri. Wagner, Young & Lauga (2014) showed that the vertical mixing induced by an ensemble of microorganisms, represented by force dipoles, at small Reynolds and Péclet numbers is very small ($\approx 8\,\%$). Here we consider the mixing induced by a Taylor swimming sheet. Interestingly, our results show that the mixing efficiencies can reach up to $40\,\%$ for thermally stratified water. Although the viscous dissipation increases with stratification as mentioned before, the bending of the streamlines induces additional vertical velocities in the fluid domain (see figure 2*b*). This causes the mass flux to increase, which consequently increases the potential energy of the fluid. As a result, we observe that the mixing efficiency increases with Ri. Wang & Ardekani (2015) also observed that mixing efficiency increases with stratification strength at low Reynolds numbers by performing fully resolved three-dimensional simulations on a suspension of squirmers swimming in thermally stratified water ($Pr = 7$). In addition to this, we observe that for lower values of diffusion ($Pr = 700$), which is the case for salt-stratified water, the mixing efficiency increases with stratification and then saturates for higher values of Ri. This indicates that the change in potential energy balances the viscous dissipation for low diffusion and higher stratification strength. The maximum mixing efficiency for salt-stratified water is about $15\,\%$. We find that the mixing efficiency is highest when the diffusion of the stratifying agent is very high ($Pr \approx 0$). We thus infer that, at low Reynolds number, a swimmer immersed in thermally stratified water will induce more mixing compared to salt-stratified water.

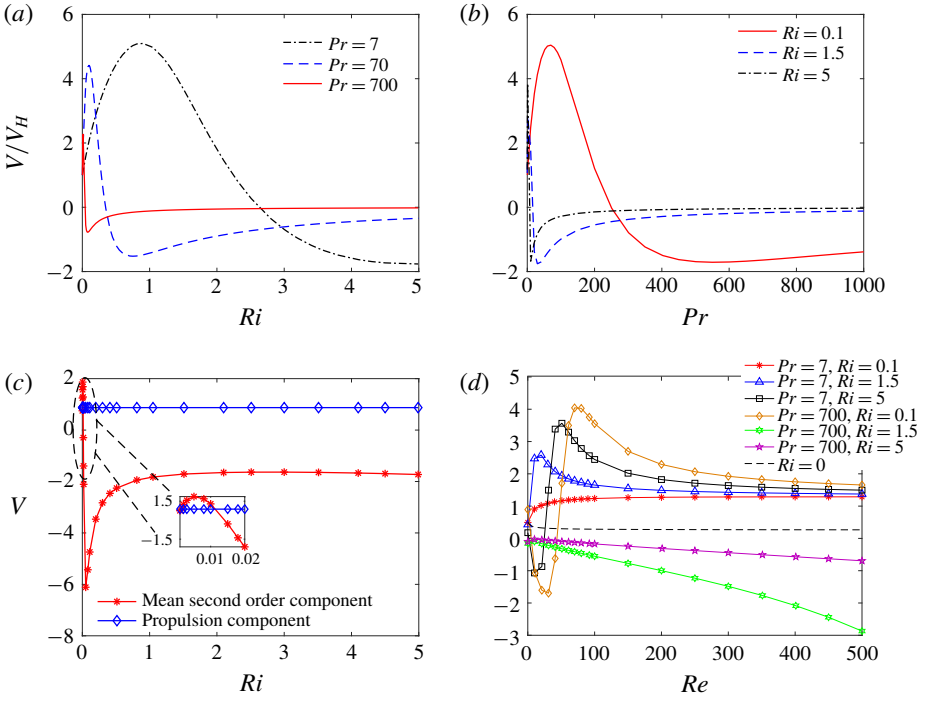

FIGURE 7. (Colour online) Variation of swimming velocity with (*a*) Richardson number and (*b*) Prandtl number, for $Re = 5$, normalized with that in a homogeneous fluid at the same Re. (*c*) Decomposition of the swimming velocity into two components for $Pr = 700$, $Re = 5$. (*d*) Variation of swimming velocity with Reynolds number.

4.2. *Finite inertia analysis*

Next, we discuss the effect of inertia in our analysis. We will analyse the effect of stratification on the same parameters that were considered for the low-Reynolds-number regime. Although our procedure is applicable for any arbitrary value of Pr, we focus our attention on the cases where diffusion is not significantly large ($Pr > 1$). These are the problems which are typically encountered in practice as mentioned before (salt-stratified water ($Pr = 700$); temperature-stratified water ($Pr = 7$)). Analysis of the influence of stratification on swimming in high-diffusion scenarios is given briefly in the Appendix.

4.2.1. *Effect of stratification on swimming velocity*

Figure 7(*a*) shows the effect of stratification on the swimming velocity for $Re = 5$. We observe that inclusion of inertia augments the swimmer's velocity for low stratification strength. For thermally induced stratification ($Pr = 7$), the maximum velocity increase is almost five times that of the homogeneous case. Further increase in stratification strength causes the velocity to decrease, ultimately leading to a direction reversal for a sufficiently high Ri. Even higher values of Ri induce a nominal increase in the velocity with the opposite swimming direction maintained. For low values of diffusion ($Pr = 700$), the velocity of the swimmer is almost zero for most values of Ri considered. This implies that strong salt stratification inhibits the vertical migration of the swimmer causing it to remain essentially stationary.

Variation with Pr also follows a similar trend, comprising a velocity peak followed by a motion reversal, eventually leading to saturation (see figure 7*b*). Interestingly, higher stratification strengths tend to completely hamper the velocity of the sheet. We thus conclude that, for moderately small values of Re, if the diffusion of the stratifying agent is very low or the stratification strength of the fluid is high, then the swimmer will not propel (see figure 7*a*,*b*). This observation is similar to the preferential aggregation of marine organisms at pycnoclines at steep density gradients reported by Harder (1968).

Similar to the Stokes regime, we find that the swimming velocity follows a trend similar to the contribution of the mean second-order velocity field developed in the fluid domain (see figure 7*c*). We also observe that the propulsion component of the velocity is almost independent of Ri. As discussed before, we know that the propulsion component of the velocity is governed by the vorticity generated in the fluid. We note that, when inertial effects are considered, the inertia-induced vorticity near the sheet crests dominates the vorticity induced due to the density gradients. Consequently, we find that stratification has a negligible influence on the propulsion component of the velocity. For a homogeneous fluid, Tuck (1968) noted that inclusion of inertia creates a second-order mean convective velocity which opposes propulsion. However, for a density-stratified fluid, we find that the second-order velocity field supports propulsion for smaller Ri, and opposes propulsion for higher density gradients (see figure 7*c*). We see that, for higher Ri, the resistance to motion dominates over the propulsion component causing the swimmer to reverse its direction of motion.

Next, we quantify the variation of the swimming velocity with Reynolds number for the cases of both temperature and salt stratification (figure 7*d*). We find that, in contrast to a homogeneous fluid, the presence of stratification causes the swimming velocity to become more sensitive to inertial effects. For thermally stratified water, the swimming velocity is independent of Re for higher Reynolds numbers and only increases with stratification. The saturation of swimming velocity at higher Re is also seen for a homogeneous fluid. This is not the case for salt stratification, where we observe that higher stratification strengths cause the swimming velocity to increase with Re, with the swimmer reversing its direction of motion for all Reynolds numbers. As explained before (figure 7*c*), this is mainly because of the dominance of the mean second-order velocity component which becomes negative for higher stratification strengths.

4.2.2. *Effect of stratification on power expenditure and swimming efficiency*

In the case of finite Re, we have

$$\boldsymbol{\nabla}\cdot\sigma = (Ri\rho')\boldsymbol{e}_y + Re\frac{\mathrm{D}\boldsymbol{u}}{\mathrm{D}t}. \tag{4.8}$$

Here, $\mathrm{D}/\mathrm{D}t$ represents the material derivative and $\boldsymbol{u} = (u, v)$ is the fluid velocity vector. Thus, unlike the Stokes regime, the work done by the fluid inertia will add to the power expended by the swimmer (see (4.3)).

As in the case of the Stokes regime, we find that with increasing stratification, the viscous dissipation in the fluid increases and the swimmer does more work in changing the potential energy of the fluid as well. Consequently, we observe that the swimmer consumes more power with increasing stratification (see figure 8*a*). We thus infer that stratification augments the power expenditure of swimmers irrespective of the importance of inertia. Figure 8(*b*) shows the effect of stratification on the

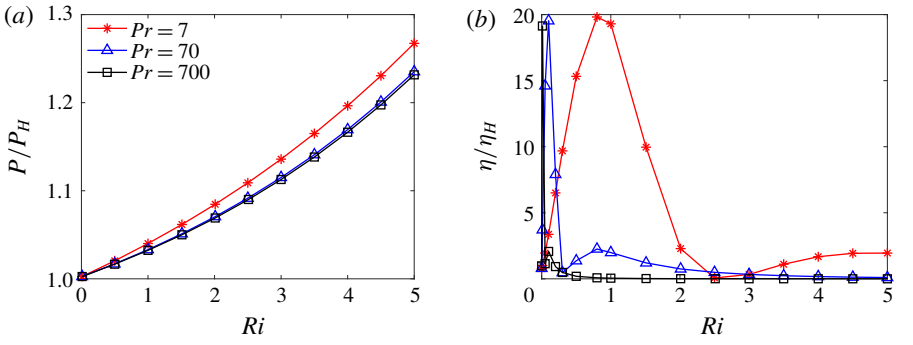

FIGURE 8. (Colour online) (*a*) Power expenditure and (*b*) hydrodynamic efficiency for $Re = 5$, normalized with respect to that in a homogeneous fluid at the same Re.

swimming efficiency for finite fluid inertia. For all values of Pr considered, the efficiency increases with Ri, reaches a peak value and then decreases. For thermal stratification, the peak efficiency is 20 times that for the homogeneous case. The trend of the swimming efficiency closely matches that for the swimmer's velocity (see figure 7*a*). This directly follows from the definition of the swimming efficiency (see (4.6)). As discussed before, for lower values of diffusion, stratification severely hampers the vertical migration of swimmers for finite fluid inertia. Consequently, we find that, for high Pr, the efficiency is zero for most values of stratification.

4.3. *Effect of stratification on mixing*

In this section, we quantify the mixing induced by a swimmer at finite Re. This analysis is relevant for the zooplankton community in oceans, which have $Re \approx O(1\text{–}100)$. We first focus on the mixing efficiency of the swimmer (refer to (4.7)). We observe that, as in the case of the Stokes regime, an increase in stratification enhances mixing efficiency of the swimmer (see figure 9*a*). However, the mixing efficiency follows a fast decay with Re (see figure 9*b*). This observation can be rationalized by considering that the viscous dissipation in the fluid increases rapidly with Re, dominating any variations in the potential energy, and ultimately leading to the decay in the mixing efficiency. This can be seen from figure 9(*c*) which shows the mean vertical viscous dissipation energy per unit volume. This observation is consistent with our knowledge derived from application of the Helmoltz minimum energy dissipation theorem, that Stokes solution has the smallest rate of viscous dissipation as compared to solutions obtained by considering finite inertia. For high Reynolds numbers ($Re > 200$), the mixing induced by the sheet is negligible for both salt and temperature stratifications. In addition to this, for salt stratification ($Pr = 700$), the mixing is insignificant for low Re as well. This implies that, for salt-stratified water, most of the power expended by the swimmer is dissipated as viscous heat for all Reynolds numbers. However, for stratification induced by temperature gradients, we find that the swimmer converts a higher fraction of the power to change the potential energy of the fluid at low Reynolds numbers, which consequently leads to higher mixing efficiencies.

Another parameter which is often used to characterize mixing is the diapycnal eddy diffusivity (K_v), which is a measure of the vertical mass flux in the fluid.

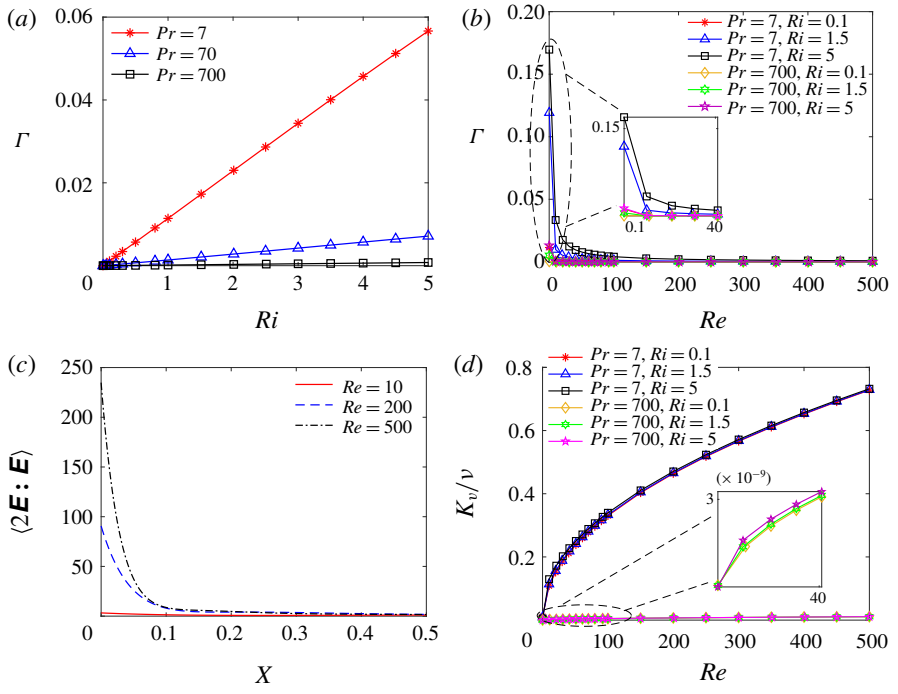

FIGURE 9. (Colour online) Variation of the mixing efficiency with (*a*) Richardson number ($Re = 5$) and (*b*) Reynolds number. (*c*) Spatial variation of vertical averaged viscous dissipation energy ($Pr = 7, Ri = 5$); $\boldsymbol{E}$ is the rate-of-strain tensor. (*d*) Variation of diapycnal eddy diffusivity with Reynolds number.

The dimensionless diapycnal eddy diffusivity is defined as (Osborn 1980)

$$\frac{K_v}{\nu} = -Re\langle\langle \rho' v\rangle\rangle. \tag{4.9}$$

Here, ρ' is the disturbed density field, v is the vertical velocity field, ν is the kinematic viscosity and $\langle\langle\cdot\rangle\rangle$ represents the average in the entire fluid domain. We calculated K_v for density-stratified water and observed the variation with Reynolds number (see figure 9*d*). We observe that the vertical mass flux induced by the swimmer due to salt stratification is negligible. For thermally stratified water ($Pr = 700$, $\nu = 10^{-6}$ m^2 s^{-1}), we find that for higher Reynolds numbers ($Re > 50$), $K_v > 10^{-7}$ m^2 s^{-1} which is the molecular temperature diffusivity in water. This implies that, for higher Re, stratification has potential to enhance mixing in the fluid. Additionally, we find that K_v increases with Reynolds number. A similar trend was observed by Wang & Ardekani (2015), by performing simulations on a suspension of squirmers in a stratified fluid by considering a volume fraction of 4 %. They also noted that the vertical mass flux is independent of stratification for $Fr \approx 20$, where Fr is the Froude number. Our results match with this observation, as it can be seen from figure 9(*d*) that increasing stratification has a negligible influence on the diapycnal eddy diffusivity at all Reynolds numbers.

5. Conclusion

We analytically obtained the swimming velocity for a self-propelling sheet immersed in a density-stratified fluid. We performed a regular perturbation to obtain this velocity up to second order of the undulation amplitude (bk). We found that, as in the case of a homogeneous fluid (Taylor 1951), the first-order component of the velocity is zero and the swimming velocity only depends on the square of the wave amplitude and the wavenumber. We analysed the influence of stratification on the swimming behaviour by considering cases of both small and finite Re.

For low Re, we found that a large density stratification in the fluid mostly hampers the vertical motion of the swimmers. This results in a swimming velocity which is less than that in a homogeneous fluid. We interestingly found that, in cases where both stratification strength and the diffusivity of the stratifying agent are low, the swimming speed is magnified and stratification supports the propulsion of the swimmer. The results in the Stokes regime are relevant for small-scale organisms in stratified environments; for example, motion of organisms such as bacteria (e.g. *Escherichia coli*, *Salmonella typhimurium*), small plankton, larvae of marine organisms and smaller sized copepods in oceanic waters. For finite inertia, we found that the swimming velocity behaviour is highly sensitive to the stratification strength, diffusion in the fluid and Reynolds number. We found that, for higher stratification strengths or low values of diffusion, the motion of the swimmer is highly restricted and it essentially remains stationary. We elucidated the similarity between this observation and the experimentally observed phenomenon of preferential aggregation of swimmers at pycnoclines for steep density gradients. The observations in the regime of finite inertia are particularly relevant for moderately sized swimmers such as zooplankton, e.g. *Euphausia pacifica* (krills) and larger sized copepods, for which the Reynolds number can be much greater than unity. The velocity behaviour in both regimes of Reynolds number is primarily governed by the mean second-order field developed in the fluid.

Stratification causes the streamlines to become vertically biased and tilt towards the denser portion of the fluid. This results in enhanced shear stresses generated in the fluid which consequently leads to an increased power expenditure by the swimmer. Moreover, the skewed streamlines cause additional vertical velocities to be developed in the fluid domain which increases the vertical mass flux. Consequently, the mixing efficiency induced by the swimmer increases with stratification. We also found that diffusion plays an important role in influencing the motility characteristics of the swimmer. A more diffusive fluid will prevent the tilting of the density contours in the presence of stratification, which more effectively counteracts the buoyancy-induced disturbances. This results in a decreased power expenditure by the swimmer and consequently leads to a higher swimming efficiency.

Increase in inertia causes a higher fraction of the power consumed by the swimmer to be expended in the form of viscous dissipation in the fluid. This leads to a decreased mixing efficiency and consequently we observe a fast decay of the mixing efficiency with Reynolds number. However, the diapycnal eddy diffusivity, which is a measure of the vertical mass flux, increases with inertia. Additionally, we found that, in both regimes of Reynolds number, a swimmer immersed in thermally stratified water leads to higher mixing efficiency and diapycnal eddy diffusivity as compared to salt-stratified water, which has negligible mixing efficiency and diapycnal eddy diffusivity in the inertial regime.

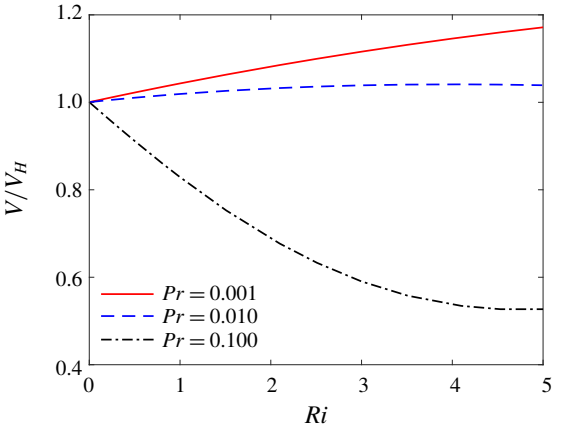

FIGURE 10. (Colour online) Effect of stratification on swimming velocity at high values of diffusion for $Re = 5$.

Acknowledgement

This publication was made possible due to support from NSF (grant nos 1700961, 1604423, and 1705371).

Appendix. Effect of stratification on swimming velocity for high diffusion, finite inertia ($Pr < 1$)

Here, we analyse the case of swimmers immersed in a highly diffusive environment (see figure 10). For $Pr = 0.001$, we see that the swimming velocity increases with stratification strength. However, with further increase in Pr, the curve becomes flatter, ultimately with the trend reversing for $Pr = 0.1$.

REFERENCES

ARDEKANI, A. M., DOOSTMOHAMMADI, A. & DESAI, N. 2017 Transport of particles, drops, and small organisms in density stratified fluids. *Phys. Rev. Fluids* **2** (10), 100503.

ARDEKANI, A. M. & STOCKER, R. 2010 Stratlets: low Reynolds number point-force solutions in a stratified fluid. *Phys. Rev. Lett.* **105** (8), 084502.

ARRIGO, K. R., ROBINSON, D. H., WORTHEN, D. L., DUNBAR, R. B., DITULLIO, G. R., VANWOERT, M. & LIZOTTE, M. P. 1999 Phytoplankton community structure and the drawdown of nutrients and CO_2 in the Southern Ocean. *Science* **283** (5400), 365–367.

BLAKE, J. R. 1971 A spherical envelope approach to ciliary propulsion. *J. Fluid Mech.* **46** (1), 199–208.

BRENNEN, C. & WINET, H. 1977 Fluid mechanics of propulsion by cilia and flagella. *Annu. Rev. Fluid Mech.* **9** (1), 339–398.

CAMPBELL, R. W. & DOWER, J. F. 2003 Role of lipids in the maintenance of neutral buoyancy by zooplankton. *Mar. Ecol. Prog. Ser.* **263**, 93–99.

CANDELIER, F., MEHADDI, R. & VAUQUELIN, O. 2014 The history force on a small particle in a linearly stratified fluid. *J. Fluid Mech.* **749**, 184–200.

CHAUDHURY, T. K. 1979 On swimming in a visco-elastic liquid. *J. Fluid Mech.* **95** (1), 189–197.

DEWAR, W. K., BINGHAM, R. J., IVERSON, R. L., NOWACEK, D. P., ST LAURENT, L. C. & WIEBE, P. H. 2006 Does the marine biosphere mix the ocean? *J. Mar. Res.* **64** (4), 541–561.

DOOSTMOHAMMADI, A., DABIRI, S. & ARDEKANI, A. M. 2014 A numerical study of the dynamics of a particle settling at moderate Reynolds numbers in a linearly stratified fluid. *J. Fluid Mech.* **750**, 5–32.

DOOSTMOHAMMADI, A., STOCKER, R. & ARDEKANI, A. M. 2012 Low-Reynolds-number swimming at pycnoclines. *Proc. Natl Acad. Sci. USA* **109** (10), 3856–3861.

DU, J., KEENER, J. P., GUY, R. D. & FOGELSON, A. L. 2012 Low-Reynolds-number swimming in viscous two-phase fluids. *Phys. Rev.* E **85** (3), 036304.

EASTMAN, J. T. 1985 The evolution of neutrally buoyant notothenioid fishes: their specializations and potential interactions in the antarctic marine food web. In *Antarctic Nutrient Cycles and Food Webs*, pp. 430–436. Springer.

ELFRING, G. J. & GOYAL, G. 2016 The effect of gait on swimming in viscoelastic fluids. *J. Non-Newtonian Fluid Mech.* **234**, 8–14.

ELFRING, G. J. & LAUGA, E. 2009 Hydrodynamic phase locking of swimming microorganisms. *Phys. Rev. Lett.* **103** (8), 088101.

ELGETI, J., WINKLER, R. G. & GOMPPER, G. 2015 Physics of microswimmers – single particle motion and collective behavior: a review. *Rep. Prog. Phys.* **78** (5), 056601.

FU, H. C., SHENOY, V. B. & POWERS, T. R. 2010 Low-Reynolds-number swimming in gels. *Eur. Phys. Lett.* **91** (2), 24002.

HARDER, W. 1968 Reactions of plankton organisms to water stratification. *Limnol. Oceanogr.* **13** (1), 156–168.

HEANEY, S. I. & EPPLEY, R. W. 1981 Light, temperature and nitrogen as interacting factor affecting diel vertical migration of dinoflagellates in culture. *J. Plankton Res.* **3** (2), 331–344.

HEUCH, P. A. 1995 Experimental evidence for aggregation of salmon louse copepodids (*Lepeophtheirus salmonis*) in step salinity gradients. *J. Mar. Biol. Assoc. UK* **75** (4), 927–939.

KATIJA, K. 2012 Biogenic inputs to ocean mixing. *J. Expl Biol.* **215** (6), 1040–1049.

KATIJA, K. & DABIRI, J. O. 2009 A viscosity-enhanced mechanism for biogenic ocean mixing. *Nature* **460** (7255), 624–626.

KATZ, D. F. 1974 On the propulsion of micro-organisms near solid boundaries. *J. Fluid Mech.* **64** (1), 33–49.

KRIEGER, M. S., DIAS, M. A. & POWERS, T. R. 2015 Minimal model for transient swimming in a liquid crystal. *Eur. Phys. J.* E **38** (8), 1–9.

LAUGA, E. 2007 Propulsion in a viscoelastic fluid. *Phys. Fluids* **19** (8), 083104.

LAUGA, E. 2016 Bacterial hydrodynamics. *Annu. Rev. Fluid Mech.* **48** (1), 105–130.

LAUGA, E. & POWERS, T. R. 2009 The hydrodynamics of swimming microorganisms. *Rep. Prog. Phys.* **72** (9), 096601.

LESHANSKY, A. M. 2009 Enhanced low-Reynolds-number propulsion in heterogeneous viscous environments. *Phys. Rev.* E **80** (5), 051911.

LIGHTHILL, M. J. 1952 On the squirming motion of nearly spherical deformable bodies through liquids at very small Reynolds numbers. *Commun. Pure Appl. Maths* **5** (2), 109–118.

MAHADEVAN, A., DASARO, E., LEE, C. & PERRY, M. J. 2012 Eddy-driven stratification initiates North Atlantic spring phytoplankton blooms. *Science* **337** (54), 54–59.

OSBORN, T. R. 1980 Estimates of the local rate of vertical diffusion from dissipation measurements. *J. Phys. Oceanogr.* **10** (1), 83–89.

PHLEGER, C. F. 1998 Buoyancy in marine fishes: direct and indirect role of lipids. *Am. Zool.* **38** (2), 321–330.

REYNOLDS, A. J. 1965 The swimming of minute organisms. *J. Fluid Mech.* **23** (2), 241–260.

SHERMAN, B. S., WEBSTER, I. T., JONES, G. J. & OLIVER, R. L. 1998 Transitions between *Aulacoseira* and *Anabaena* dominance in a turbid river weir pool. *Limnol. Oceanogr.* **43** (8), 1902–1915.

SIMONCELLI, S., THACKERAY, S. J. & WAIN, D. J. 2017 Can small zooplankton mix lakes? *Limnol. Oceanogr.* **2** (5), 167–176.

STRICKLER, J. R. 1975 Swimming of planktonic cyclops species (copepoda, crustacea): pattern, movements and their control. In *Swimming and Flying in Nature*, pp. 599–613. Springer.

SZNITMAN, J., PUROHIT, P. K., KRAJACIC, P., LAMITINA, T. & ARRATIA, P. E. 2010 Material properties of *Caenorhabditis elegans* swimming at low Reynolds number. *Biophys. J.* **98** (4), 617–626.

TAYLOR, G. 1951 Analysis of the swimming of microscopic organisms. *Proc. R. Soc. Lond.* A **209** (1099), 447–461.

THORPE, S. A. 2005 *The Turbulent Ocean*. Cambridge University Press.

TUCK, E. O. 1968 A note on a swimming problem. *J. Fluid Mech.* **31** (02), 305–308.

VISSER, A. W. 2007 Biomixing of the oceans? *Science* **316** (5826), 838–839.

VISSER, A. W. & JÓNASDÓTTIR, S. H. 1999 Lipids, buoyancy and the seasonal vertical migration of *Calanus finmarchicus*. *Oceanography* **8**, 100–106.

WAGNER, G. L., YOUNG, W. R. & LAUGA, E. 2014 Mixing by microorganisms in stratified fluids. *J. Mar. Res.* **72** (2), 47–72.

WANG, S. & ARDEKANI, A. M. 2015 Biogenic mixing induced by intermediate Reynolds number swimming in stratified fluids. *Sci. Rep.* **5**, 17448.

YEN, J., BROWN, J. & WEBSTER, D. R. 2003 Analysis of the flow field of the krill, *Euphausia pacifica*. *Mar. Freshw. Behav. Physiol.* **36** (4), 307–319.

YICK, K. Y., TORRES, C. R., PEACOCK, T. & STOCKER, R. 2009 Enhanced drag of a sphere settling in a stratified fluid at small Reynolds numbers. *J. Fluid Mech.* **632**, 49–68.